

An Analysis of the Performance of Secant – Shaped Porous Slider Bearing Lubricated with Couple Stress Fluid under the Effect of Slip Velocity and Squeeze Velocity

Biradar Kashinath (Rtd)¹ and Adinatha C. Upadhya²

¹Department of Mathematics, Government First Grade College, Sedam, Karnataka, India.

²Department of Mathematics, Sangolli Rayanna First Grade Constituent College, Belagavi, Karnataka, India

Article History:

Received: 12-01-2025

Revised: 15-02-2025

Accepted: 01-03-2025

Abstract: An attempt has been made to study the analysis on the performance of secant – shaped porous slider bearing lubricated with couple stress fluid considering slip velocity and squeeze velocity. In the present study, we investigate the characteristics of the bearing with the impact of permeability and couple stresses by considering slip velocity and squeeze velocity. Based on Stokes constitutive equations for couple stress fluids and Darcy's law for porous medium the modified Reynolds type equation is derived. The modified Reynolds equation is solved analytically and closed form expressions are obtained for the fluid film pressure, load carrying capacity, frictional force and centre of pressure. Computed values of dimensionless load capacity of bearing, friction force on the moving slider, coefficient of friction and the position of centre pressure were displayed in graphical form. The figures are presented here tend to establish that the use of couple stress fluid as a lubricant increases the load carrying capacity and decreases the coefficient friction. The load capacity, friction and coefficient of friction decreased when the slip parameter increased. But, the load capacity as well as friction decreased and the coefficient of friction increased when the permeability the parameter increased.

Keywords: Porous, Squeeze film, Couple stress, Slider bearings, Slip velocity.

1. Introduction

Nowadays, squeezing film technology is widely observed in applications of engineering practices such as aircraft engines, automotive engines, machine tools, turbo chemistry, dampers, human joints etc. The squeeze film behaviour arises from the phenomenon of two lubricated surfaces approaching each other with the normal velocity. Because the viscous lubricant contained between the two surfaces cannot be instantaneously squeezed out because it takes a certain for these surfaces to come into contact. Since the viscous lubricant has extrusion resistance pressure is built up during that interval and the load is then supported by the lubricant film.

Bearing's are one of the most commonly used machine components because of their advantages in comparison with rolling bearings. In general, slider bearing production is simple which leads to lower. Self-lubricated slider bearings are useful in several applications. There are two types of self-lubricated bearings. Namely, slider bearings working without any lubricants and slider bearings containing lubricants either in special storage or in their material such as porous metal bearings. A porous medium is a matter that contains many small holes distributed throughout the matter. The porous bearings do not need an external supply of lubricant during their operation. Therefore their structures are simple

and reduce costs for this reason the study of porous bearings has attracted the attention of several investigators and a porous bearing contains a porous material filled with lubricating oil so that the bearing requires no further lubrication during the whole life of the machine. Self-lubricated bearings or oil-retaining bearings exhibit this feature. Self-lubricating porous bearings have the advantage of a high production rate because of short sintering time. Graphite is added to enhance the self-lubricating property of the bearings. The applications of porous metal bearings are small motors, vacuum cleaners, shaving machines, tape recorders, coffee grinders, water pumps, record players, generators and distributors. Morgan and Cameron [1] who first gave an analytical survey of the study of porous bearings with the aid of hydrodynamic conditions. Wu [2] investigated the squeeze film behaviour of porous annular discs. Sparrow *et.al.* [3] analysed the effect of velocity slip on porous walled squeeze films. Prakash and Vij [4] investigated the hydrodynamic lubrication of porous slider bearings. Murti [5] studied an infinitely wide porous slider bearing. Patel and Gupta [6] analysed the problem of inclined slider bearing by considering slip velocity at the porous boundary. Bujurke *et.al.* [7] theoretically analysed the couple stress fluid effect on porous slider bearing and later on the performance of a secant-shaped porous slider bearing lubricated with couple stress fluids, by Bujurke *et.al* [8]. Naduvinmani *et.al.* [9] studied the effect of roughness on hydromagnetic squeeze film between porous rectangular plates. In all these studies the lubricant was assumed to be Newtonian fluid. However, the Newtonian fluid constitutive approximation is not a satisfactory approach for practical applications. Many researchers worked to overcome this limitation and found that by adding some amount of long-chained polymers to Newtonian fluid, the desirable lubricant can be obtained. Many theories were proposed to represent the use of non-Newtonian fluids. Among these, micro continuum theory is the simplest generalization of the classical theory of fluids proposed by Stokes [10], which allows for polar effects such as the presence of couple stresses, body couples and non-symmetric tensors. The effects of couple stresses are quite large for large values of dimensional material constant l . It varies for different liquids depending upon the molecular dimensions of the liquid. Therefore couple stresses are in-noticeable magnitudes in liquids with very large molecules. These fluids with effective magnitudes of material constant l are known as couple stress fluids. The concept of couple stress fluids was also applied to porous bearings by Hwang *et.al.* [11]. They concluded that as the value of the porous wall thickness increases, it increases the load capacity of the bearing. Also, when the inclination of the slider increases, the load-carrying capacity increase with a decrease in the friction parameter.

Because of the use of squeeze film slider bearings in clutch plates, automobiles, transmission and domestic appliances many investigators Sparrow *et.al.*[12], Prakash and Vij [13], Bhat and Patel [14], Puri *et.a.* [15] dealt with the problem of a squeeze film slider bearing. Slider bearing has been studied in various film shapes by many investigators such as Pinkus and Sternlicht [16], Bagci and Singh [17], Hamrock [18], Naduvinamani N.B, *et.al.* [19], Shah and Bhat [20], Dipak *et.al.*[21].

Considering the flexibility of porous bearings and their applications in this paper, an attempt is made for an investigation of the analysis on the performance of secant-shaped porous slider bearing lubricated with couple stress fluid considering slip velocity and squeeze velocity.

2. Mathematical formulation and Solution of the Problem

The diagram as shown in Figure 1.1 represents the secant-shaped porous slider bearing of uniform thickness H backed by a solid wall. It has a length of L and breadth of B with $L < B$. The porous bearing's lower surface is at rest while the upper solid surface is in motion with a uniform velocity U in the x -direction including the effect of squeezing action $\dot{h} = \frac{\partial h}{\partial t}$, where t seconds.

A mathematical expression for the film thickness h is given by,

$$h = h_1 \sec \left\{ \frac{\pi(L-x)}{2L} \right\}, \quad 0 < x \leq L \tag{1}$$

where h_1 is the minimum film thickness.

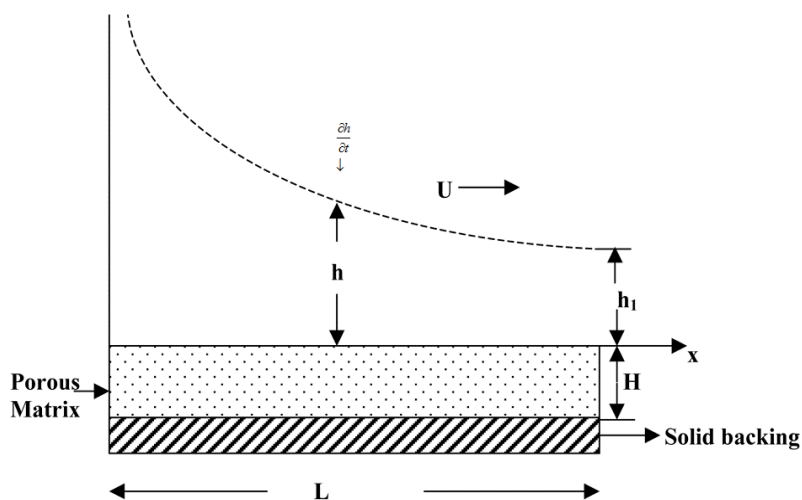


Figure 1.1 Geometrical configuration of secant-shaped porous slider bearing bearings with squeeze velocity \dot{h}

Under the usual assumptions of hydrodynamic lubrication, the equations of motion proposed by Stokes (1966) for a couple stress fluids in the film region take the form (Naduvinimani *et.al.* 2003),

$$\frac{\partial u}{\partial x} + \frac{\partial v}{\partial y} = 0 \tag{2}$$

$$\mu \frac{\partial^2 u}{\partial y^2} - \eta \frac{\partial^4 u}{\partial y^4} = \frac{\partial p}{\partial x} \tag{3}$$

$$\frac{\partial p}{\partial y} = 0$$

(4)

The modified version of Darcy's law for isotropic porous materials governs the flow of couple stress fluid in a porous matrix.

$$\vec{q}^* = \frac{-k}{\mu(1-\beta)} \nabla p^* \tag{5}$$

where, $\vec{q}^* = (u^*, v^*)$, $\beta = \frac{\eta}{\mu\kappa}$ and the parameter κ is the permeability of the porous material and is

known as pore size and β is the ratio of microstructure size to the pore size. If $\left(\frac{\eta}{\mu}\right)^{1/2} \approx \sqrt{k}$ i.e., $\beta \approx 1$

then the lubricant's microstructure additives obstruct the pores in the porous layer, reducing Darcy flow through the porous matrix. When the size of the microstructure is very small in comparison to the size of the pores, $\beta \ll 1$ the additives percolate into the porous matrix. The limit $\beta \rightarrow 0^+$ equation (5) reduces to the usual Darcy's law. Laplace's equation is satisfied by the pressure formed by continuity in the porous area:

$$\frac{\partial^2 p^*}{\partial x^2} + \frac{\partial^2 p^*}{\partial y^2} = 0 \tag{6}$$

The relevant boundary conditions for the velocity components are:

(i) At the upper solid surface ($y = h$)

$$u = U, \quad \frac{\partial^2 u}{\partial y^2} = 0 \tag{7a}$$

$$v = \frac{dh}{dt} \tag{7b}$$

(ii) At the lower surface ($y = 0$)

$$u = \frac{1}{s} \frac{\partial u}{\partial y} \Big|_{y=0}, \quad \frac{\partial^2 u}{\partial y^2} = 0 \tag{8a}$$

$$v = v^* \tag{8b}$$

where, $s = (\alpha/\sqrt{k})$ is the slip parameter and α is the dimensionless slip constant.

Solving equation (2) with boundary conditions (7a) and (8a) the velocity components u can be derived as follows

$$u = \frac{1}{2\mu} \cdot \frac{\partial p}{\partial x} \left[(y-h) \left\{ y + \frac{h}{3} \xi_1 - 2\xi_0 \frac{\tanh\left(\frac{lh}{2}\right)}{l} \right\} + \frac{2}{l^2} \left\{ 1 - \frac{\cosh\left[\frac{(ly-lh)}{2}\right]}{\cosh\left[\frac{lh}{2}\right]} \right\} \right] + \left(\frac{1}{1+sh} + \frac{ys}{1+sh} \right) U \tag{9}$$

where, $\xi_0 = \frac{1}{1+sh}$, $\xi_1 = \frac{3}{1+sh}$, $l = \left(\frac{\eta}{\mu}\right)^{1/2}$

Integrating equation (6) with respect to y over the porous layer thickness H and applying the boundary conditions $\frac{\partial p^*}{\partial y} = 0$ at $y = -H$, we obtain:

$$\left(\frac{\partial p^*}{\partial y}\right)_{y=0} = -\int_{y=0}^{-H} \frac{\partial^2 p^*}{\partial x^2} dy \tag{10}$$

Applying the pressure $p = p^*$ continuity condition of the interface $y=0$ of the porous matrix and fluid film and assuming a very thin porous layer thickness H , equation (10) reduces to:

$$\left(\frac{\partial p^*}{\partial y}\right)_{y=0} = -H \frac{\partial^2 p^*}{\partial x^2} \tag{11}$$

Substituting the expressions for u in the continuity equation (2) and integrating across the fluid film thickness and using the boundary conditions (7b) and (8b) for v gives the nonlinear modified Reynold's equation is:

$$\frac{\partial}{\partial x} \int_0^h u dy + (v_{y=h} - v_{y=0}) = 0 \tag{12}$$

yields,

$$\frac{\partial}{\partial x} \left\{ \left(f(h, s, l) + \frac{12KH}{1-\beta} \right) \frac{\partial p}{\partial x} \right\} = 6\mu U \frac{d}{dx} \left(\frac{h(2+hs)}{1+sh} \right) + 12\mu V \tag{13}$$

where,

$$f(h, s, l) = h^3(1 + \xi_1) - 6h^2\xi_0 \frac{\tanh\left(\frac{lh}{2}\right)}{l} - \frac{12}{l^2} \left(h - \frac{2 \tanh\left[\frac{lh}{2}\right]}{l} \right), \quad v_{y=h} = V = \frac{dh}{dt} = \dot{h}$$

Using the following non-dimensional parameters in (13), we get

$$x^* = \frac{x}{L}, \quad h^* = \frac{h}{h_1}, \quad p^* = \frac{ph_1^2}{\mu UL}, \quad S = -\frac{2LV}{Uh_1}, \quad \psi = \frac{kH}{h_1^3}, \quad \tau = lh_1, \quad s^* = sh_1, \quad h^* = \sec\left(\frac{\pi(1-x^*)}{2}\right)$$

Equation (13) takes the form:

$$\frac{\partial}{\partial x^*} \left\{ \left(f^*(h^*, s^*, \tau) + \frac{12\psi}{1-\beta} \right) \frac{\partial p^*}{\partial x^*} \right\} = \frac{dG}{dx^*} \tag{14}$$

where,

$$\xi_0^* = \frac{1}{1+s^*h^*}; \quad \xi_1^* = \frac{3}{1+s^*h^*}; \quad G = 6 \left(\frac{2h^* + s^*h^{*2}}{1+s^*h^*} \right) - 6x^*S,$$

$$f^*(h^*, s^*, \tau) = h^{*3} (1 + \xi_1^*) - 6 h^{*2} \xi_0^* \frac{\tanh(\tau h^*/2)}{\tau} - \frac{12}{\tau^2} \left(h^* - \frac{2 \tanh(\tau h^*/2)}{\tau} \right)$$

Equation (14) is known as the dimensionless Reynold’s equation. Because the pressure at the boundaries of the slider bearing is negligible compared to the internal pressure.

The pressure field boundary conditions are:

$$p^* = 0 \text{ at } x^* = 0, 1 \text{ (Ambient pressure)} \tag{15}$$

Integrating the equation of (14) with respect to x^* :

$$\frac{\partial p^*}{\partial x^*} = \frac{G - Q}{\left(f^*(h^*, s^*, \tau) + \frac{12\psi}{1 - \beta} \right)} \tag{16}$$

where Q is the constant integration

Solving equation (16) subject to the boundary conditions (15) which gives the dimensionless film pressure p^* is obtained as:

$$p^* = \int_{x^*=0}^{x^*} \frac{G - Q}{f(h^*, s^*, \tau) + \frac{12\psi}{(1 - \beta)}} dx^* \tag{17}$$

where,

$$Q = \frac{\int_{x^*=0}^1 \frac{G}{f(h^*, s^*, \tau) + \frac{12\psi}{(1 - \beta)}} dx^*}{\int_{x^*=0}^1 \frac{1}{f(h^*, s^*, \tau) + \frac{12\psi}{(1 - \beta)}} dx^*}$$

The load carrying capacity W^* are given in dimensionless form by, $W^* = \frac{Wh_0^2}{\mu UL^2} = \int_0^1 p^* dx^*$

(18) The component of the stress tensor required to calculate the frictional force is,

$$\tau_{yx} = \mu \left(\frac{\partial u}{\partial y} \right)_{y=h} - \eta \left(\frac{\partial^3 u}{\partial y^3} \right)_{y=h} \tag{19}$$

The frictional force F per unit width on the bearing surface is given by,

$$F = \int_0^L (\tau_{yx})_{y=h} dx \tag{20}$$

Use of expression (9) for u in equation (17) and substituting it in equation (18), gives frictional force which after non-dimensional becomes

$$F^* = \int_0^1 \left\{ \frac{s^*}{(1+s^*h^*)} + \frac{\left(h^* (2+s^*h^*) - \left(2/\tau \tanh\left(\frac{\tau h^*}{2}\right) \right) \right) \{G-Q\}}{2(1+s^*h^*) \left\{ f^*(h^*, s^*, \tau) + \frac{12\psi}{1-\beta} \right\}} \right\} dx^* \tag{21}$$

The coefficient of friction is

$$f^* = \frac{F^*}{W^*} \tag{22}$$

The location of the centre of pressure, where the resultant force acts are:

$$x^* = \frac{1}{W^*} \int_0^1 p^* \cdot x^* dx^* \tag{23}$$

3. Results and discussions

In this present paper the analysis on the performance of secant-shaped porous slider bearing lubricated with couple stress fluid considering slip velocity and squeeze velocity is analysed with the aid of various dimensionless parameters viz; the couple stress parameter, the permeability parameter, slip parameter and the squeeze velocity.

3.1 Fluid film pressure

The graphs illustrated in Figure 1.2 to Figure 1.4 represent variation in non-dimensional pressure p^* against x^* with the effect of squeeze velocity $\dot{h} \neq 0$. Figure 1.2 shows the variation of non-dimensional pressure p^* with x^* for different values of τ with $\beta = 0.3$, $\psi = 0.001$, $s^* = 0.3$, $S = 0.5$. It is observed that the effect of couple stress is to increase non-dimensional pressure p^* as compared to the corresponding Newtonian case ($\tau = \infty$) in the presence of squeeze velocity. Figure 1.3 shows the variation of non-dimensional pressure p^* with τ for different values of s^* with $\beta = 0.3$, $\psi = 0.001$, $\tau = 12.5$, $S = 0.5$. It is found that the effect of velocity slip is to decrease dimensionless p^* as compared to no slip case ($s^* = \infty$). Figure 1.4 shows the variation of non-dimensional pressure p^* with x^* for different values of ψ with $\beta = 0.3$, $\tau = 12.5$, $s^* = 0.3$, $S = 0.5$. It is seen that the p^* decreases with increasing values of permeability ψ . It is also interesting to note that the point of maximum pressure x_{max}^* shifts towards the inlet edge for increasing values of ψ .

3.2 Load carrying capacity

The graphs illustrated in Figure 1.5 to Figure 1.6 represent variation in non-dimensional load W^* against τ with the effect of squeeze velocity $\dot{h} \neq 0$. Figure 1.5 shows the variation of non-dimensional load carrying capacity W^* with couple stress parameter τ for different values of ψ with $\beta = 0.3$, $s^* = 0.3$, $S = 0.5$. A significant increase in W^* observed as compared to the corresponding to the Newtonian case ($\tau = \infty$) in the presence of squeeze velocity. Furthermore, the significant reduction in W^* is observed with increasing values of permeability ψ . Figure 1.6 shows the variation of non-dimensional load

carrying capacity W^* with couple stress parameter τ for different values of s^* with $\beta=0.3$, $\psi=0.001$, $S=0.5$. It is seen that the effect of velocity slip is to decrease dimensionless W^* as compared to no slip case ($s^*=\infty$). Figure 1.7 shows the variation of non-dimensional load W^* against τ for different values of h with $\beta=0.3$, $l^*=0.5$, $s^*=0.3$, $\psi=0.001$, $h_0=0.02$, $L=0.005$ and $U=1.0$. It is found that W^* increases considerably in the presence of squeeze velocity.

3.3 Frictional force

The graphs illustrated in Figure 1.8 to Figure 1.9 represent variation in non-dimensional load F^* against τ with the effect of squeeze velocity $h \neq 0$. Figure 1.8 shows the variation of non-dimensional frictional force, F^* with τ for different values of ψ with $\beta=0.3$, $\psi=0.001$, $S=0.5$. It is seen that a marginal increase in F^* is observed as compared to the corresponding to the Newtonian case ($\tau=\infty$) for all values of ψ . Furthermore, a reduction in F^* is observed for increasing values of permeability ψ . Figure 1.9 shows the variation of non-dimensional frictional force F^* with τ for different values of s^* with $\beta=0.3$, $\psi=0.001$, $S=0.5$. It is seen that the effect of velocity slip is to decrease dimensionless friction F^* as compared to no slip case ($s^*=\infty$).

3.4 Coefficient of friction

The graphs illustrated in Figure 1.10 to Figure 1.11 represent variation in non-dimensional load f^* against τ with the effect of squeeze velocity $h \neq 0$. Figure 1.10 shows the variation of the non-dimensional coefficient of friction f^* with τ for different values of ψ with $\beta=0.3$, $\psi=0.001$, $S=0.5$. It is interesting to observed that the drastic reduction in coefficient of friction f^* is observed as compared to the corresponding to the Newtonian case ($\tau=\infty$) for all values of ψ . However, a significant increase in f^* is observed for increasing values of permeability ψ . Figure 1.11 shows the variation of the non-dimensional coefficient of friction f^* with τ for different values of s^* with $\beta=0.3$, $\psi=0.001$, $S=0.5$. It is observed that the effect of velocity slip is to decrease f^* as compared to no slip case ($s^*=\infty$).

3.5 Centre of pressure

The graphs illustrated in Figure 1.12 to Figure 1.13 represent variations in the non-dimensional centre of pressure x^* against couple stress parameter τ with the effect of squeeze velocity $h \neq 0$. It is observed that the centre of pressure x^* shifts towards the outlet edge when the couple stress parameter τ decreases. It is also found that the centre of pressure x^* shifts towards the inlet edge when the increasing values of ψ with given s^* .

4. Conclusions

In this paper an analysis of the performance of secant-shaped porous slider bearing lubricated with couple stress fluid considering slip velocity and squeeze velocity are investigated. From this investigation the following conclusions have been made.

- Pressure increases with an increase in couple stress parameters but the pressure decreases with increases in the value of permeability.

- The use of classical lubricant blended with microstructure additives provides an increased load-carrying capacity and decreased coefficient of friction.
- The Load carrying capacity decreases with increases in the value of permeability.
- The centre of pressure shifts towards the outlet edge when the couple stress parameter decreases.
- The centre of pressure shifts towards the inlet edge for increasing values of permeability parameters.

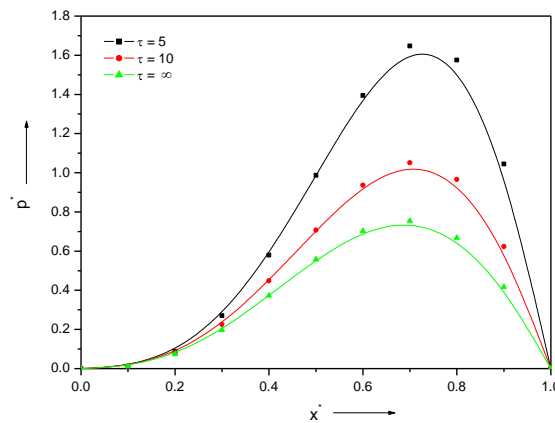


Figure 1.2 Variation of non-dimensional pressure p^* with x^* for different values of couple stress parameter τ with $S=0.5, \beta=0.3, s^*=0.3, \psi=0.001$.

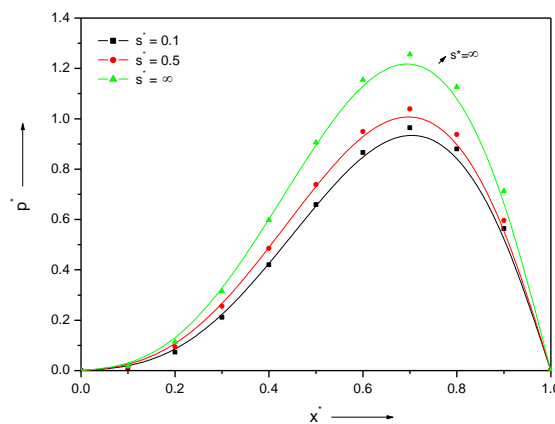


Figure 1.3 Variation of the non-dimensional pressure p^* with x^* for different values s^* with $S=0.5, \beta=0.3, \psi=0.001$.

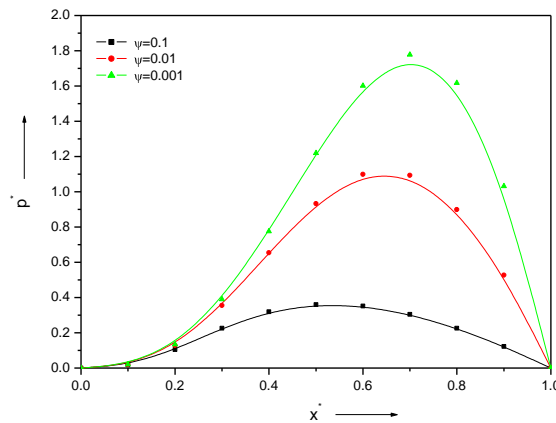


Figure 1.4 Variation of non-dimensional pressure p^* with x^* for different values of permeability parameter ψ with $S=0.5$, $\beta=0.3$, $s^*=0.3$, $\tau=12.5$.

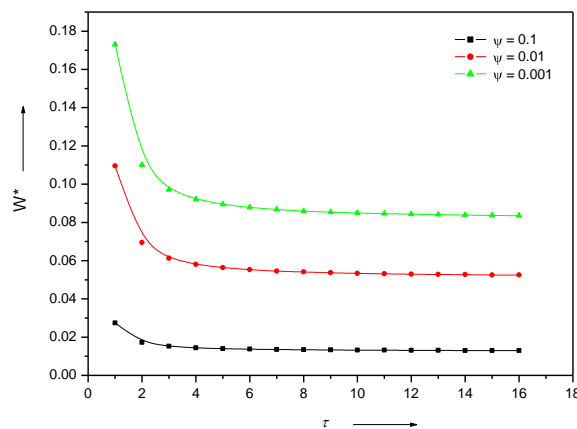
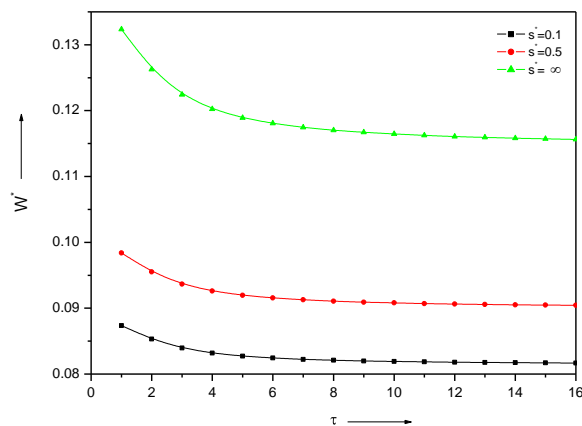


Figure 1.5 Variation of non-dimensional load W^* with τ for different values ψ , with $S=0.5$, β



$=0.3$, $s^*=0.3$.

Figure 1.6 Variation of the non-dimensional load W^* with τ for different values s^* with $S=0.5$, $\beta=0.3$, $\psi=0.001$

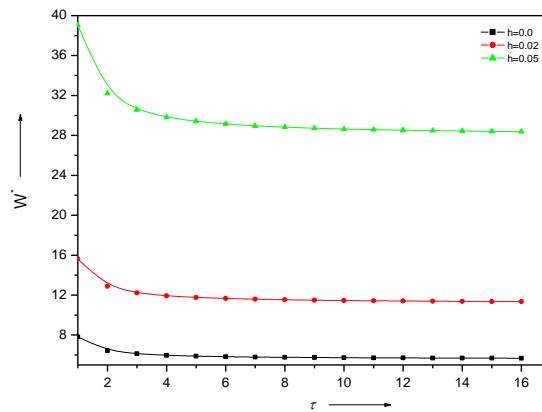


Figure 1.7 Variation of the non-dimensional load W^* with τ for different values \hat{h} with $s^* = 0.3$, $\beta = 0.3$, $\psi = 0.001$, $h_0 = 0.02$, $L = 0.005$ and $U = 1.0$

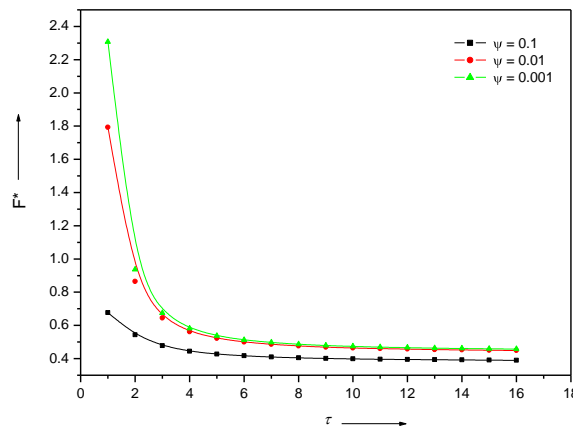


Figure 1.8 Variation of the frictional force F^* with τ for different values ψ with $S = 0.5$, $\beta = 0.3$, $s^* = 0.3$

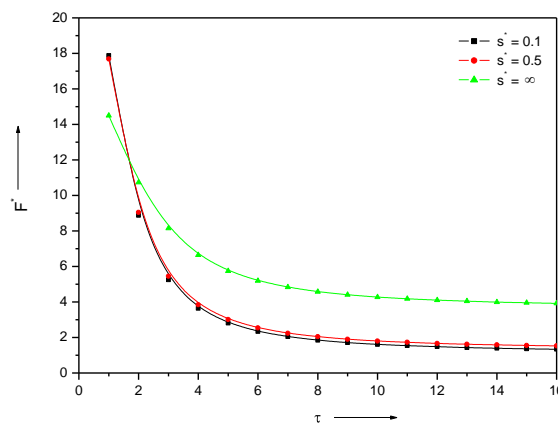


Figure 1.9 Variation of the non-dimensional frictional force F^* with τ different values s^* with $S = 0.5$, $\beta = 0.3$, $\psi = 0.001$

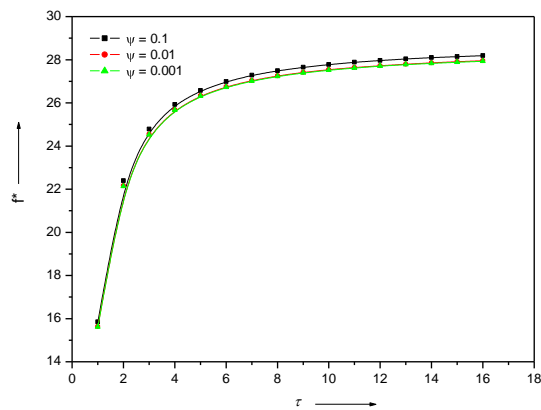


Figure 1.10 Variation of non-dimensional coefficient of friction f^* with τ for different values ψ with $S=0.5$, $\beta=0.3$, $s^*=0.3$

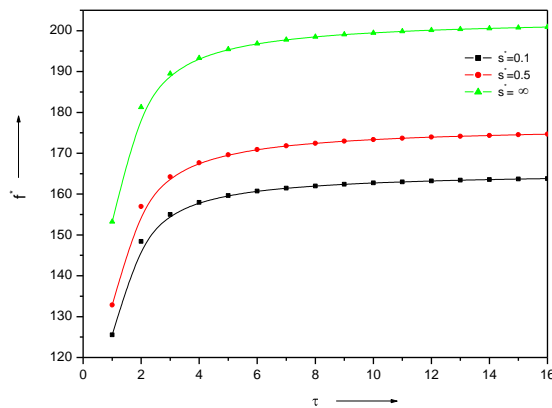


Figure 1.11 Variation of non-dimensional coefficient of friction f^* with for different values s^* with $S=0.5$, $\beta=0.3$, $\psi=0.001$

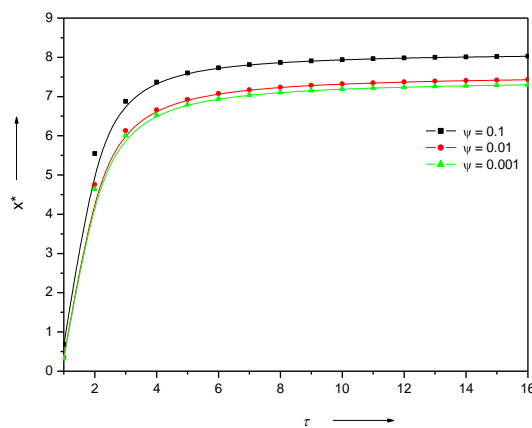


Figure 1.12 Variation of the non-dimensional centre of pressure x^* with τ for different values ψ with $S=0.5$, $\beta=0.3$, $s^*=0.3$

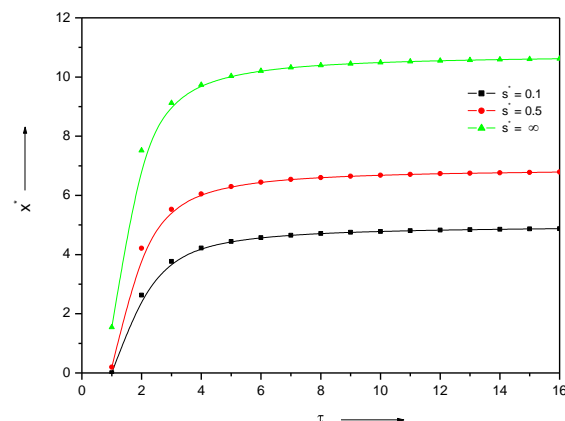


Figure 1.13 Variation of the non-dimensional centre of pressure x^* with τ for different values s^* with $S=0.5, \beta=0.3, \psi=0.001$

References

- [1] Cameron A. and, Morgan V.T.,1962, Critical conditions for hydrodynamic lubrication of porous metal bearings, Proceedings of the institution of Mechanical Engineers, Vol. 176 No. 28, pp 761-770.
- [2] H. Wu, 1970, Squeeze – film behaviour for porous annular disks, Journal of Lubrication Technology, Trans. ASME, Series F, 92(4) ,593-596.
- [3] E.M. Sparrow, G.S. Beavers, I.T. Hwang, 1972,Effect of velocity slip on porous walled squeeze films, Journal of Lubrication Technology 94 , 260-265.
- [4] J. Prakash, S.K. Vij,1973,Hydrodynamic lubrication of a porous slider, Journal of Mechanical Engineering Science 15 , 232-234.
- [5] Murti and P.R.K.,1974, Analysis of Porous Slider Bearings, Wear,28,1,131-134.
- [6] Patel K.C. and GuptaJ.L.,1983, Hydrodynamic Lubrication of a Porous Slider Bearing with Slip Velocity, Wear , 85,3, 309-317.
- [7] N.M. Bujurki, H.P. Patil and S.G. Bhavi,1990, Porous slider bearing with couple stress field, Acta-mechanica 85,99-113.
- [8] N.M. Bujurki , N.B. Naduvinmani and S.S. Benchalli, 2003,Secant –shaped porous slider bearing lubricated with couple stress fluids, Industrial Lubrication and Tribology 57/4 ,155-160.
- [9] Naduvinamani N.B., Fathima S.T. and Salma Jamal, 2010, Effect of roughness on hydromagnetic squeeze films between porous rectangular plates, Tribology International vol.43(11), P2145-2151.
- [10] V. K. Stokes,1966, Couple Stresses in fluids, Phy. Fluids, 9, 1709-1715.
- [11]Hwang CC, Lin JR, Yang RF,1996, Lubrication of long porous slider bearings, (use of the brinkman extended darcy model), Jsme International Journal, Series B: Fluids And Thermal Engineering, 39,141-148.
- [12]Sparrow. E.M., Beavers G.S. and Hwang I.T.,1972, Effect of velocity slip on porous walled squeeze films. J.Lubr. Technol, 94,260-265.

- [13] Prakash J. and Vij S.K., 1973, Load capacity and time height relation for squeeze films between porous plates. *Wear* 24, 300-315.
- [14] Bhat M.V. and Patel C.M., 1981, The squeeze film in an inclined porous slider bearing, *Wear*, vol. 66, pp. 189-93.
- [15] Puri V.K. and Patel C.M., 1982, The squeeze film in a porous composite slider bearing. *Wear*, 70(2), pp 197-206.
- [16] Pinkus O and Sternlicht B., 1961, *Theory of hydrodynamic lubrication*, Mc Graw-Hill, New York, NY.
- [17] Bagci C. and Singh, 1983, Hydrodynamic lubrication of finite slider bearing; Effect of one dimensional film shape and their computer aided optimum designs, *ASLE Trans. J. Lub. Tech.* Vol 105, pp 48-66.
- [18] Hamrock B.J., 1994, *Fundamentals of fluid film lubrication* Mc Graw-Hill, New York NY.
- [19] Naduvinamani N.B., Fathima S.T. and Hiremath P.S., 2003, Hydrodynamic lubrication of rough slider bearing with couple stress fluids, *Tribology International*, Vol. 26 No. pp 949-959
- [20] Shah R.C. and Bhat M.V., 2003, Porous secant shaped slider bearing with slip velocity lubricated by ferrofluid, *Industrial Lubr. and Trib* 55, 113-115.
- [21] Dipak A Patel, Manisha J. Atri and Dilp B. Patel, 2021 Performance of hydrodynamic porous slider bearing with water based magnetic fluid as a lubricant; Effect of slip and Squeeze velocity, *journal of scientific and Industrial Research*, Vol. 80,, pp . 508-512.